## In Situ Cryogenic Cooling, Electric Biasing, and 4D-STEM of the 1T-TaS2 Charge Density Wave Transition

James L Hart, Saif Siddique, Noah Schnitzer, Stephen Funni, Lena F Kourkoutis, Judy J Cha

DECTRIS

ARINA with NOVENA
Fast 4D STEM



DECTRIS NOVENA and CoM analysis of a magnetic sample.

Sample courses: Dr. Christian Liebscher, Max-Planck-Institut für Eisenforschung GmbH.

## Downloaded from https://academic.oup.com/mam/article/30/Supplement\_1/ozae044.673/7719846 by Cornell University user on 12 September 2024

**Meeting-report** 

## In Situ Cryogenic Cooling, Electric Biasing, and 4D-STEM of the 1T-TaS<sub>2</sub> Charge Density Wave Transition

James L Hart<sup>1,4</sup>, Saif Siddique<sup>1</sup>, Noah Schnitzer<sup>1</sup>, Stephen Funni<sup>1</sup>, Lena F Kourkoutis<sup>2,3</sup>, and Judy J Cha<sup>1,\*</sup>

While quantum materials are promising for myriad applications, their implementation is hindered by a poor understanding of their nanoscale structure. Most commonly these materials are studied with X-ray or neutron scattering methods, which only possess µm scale spatial resolution, or scanning probe methods, which are unable to probe any sub-surface features. Thus, cryogenic (scanning) transmission electron microscopy – aided by 4D-STEM and improved *in situ* holders – is an increasingly powerful method for the investigation of quantum materials.

Here we study the prototypical quantum material 1T- $TaS_2$ . At low temperature,  $TaS_2$  exhibits a commensurate (C) charge density wave (CDW) structure, wherein 13 Ta atoms bunch together forming a Star of David (Fig. 1a), and the stars organize in a hexagonal lattice with long-range order (Fig. 1b). Above  $\sim 200$  K, the C CDW phase transitions to a nearly commensurate (NC) phase, which is characterized by phase slips in the CDW packing, yielding a local CDW domain size of  $D \sim 10$  nm (Fig. 1c). The C to NC phase transition drives a large insulator-to-metal transition, which is promising for device applications. At present, our understanding of how the C to NC CDW transition evolves in real-space is lacking. Answering this question may enable improved control of the CDW phase transition and improved device performance.

We study the TaS<sub>2</sub> CDW transition using a FEI Titan Themis operated at 120 kV, an EMPAD-G2 detector for 4D-STEM, and a HennyZ holder which allows variable temperature analysis from  $\sim$ 110 – 1000 K [1]. Using scotch tape mechanical exfoliation and a PPC stamp, we transfer a  $\sim$ 60 nm thick TaS<sub>2</sub> flake onto an *in situ* chip. The chip has 2 Pt electrodes for biasing and a through-hole for STEM analysis (Fig. 1d and 1e).

To begin the STEM experiment, we cool the flake to the base temperature ( $\sim$ 110 K) to access the C CDW phase. We then slowly increase the sample temperature, measuring the sample resistance and collecting 4D-STEM datasets every few K. The resistance versus temperature data is shown in Fig 1g; an abrupt transition is observed at  $\sim$ 200 K, indicative of the CDW transition. To process the 4D-STEM data, we fit the position of every Bragg and CDW satellite peak. We then extract the CDW q vector and the Bragg lattice vector a\* (Fig. 1f). Based on the incommensurability of q and a\*, we calculate the wavelength of their moire pattern, which defines the CDW domain size D [2]. For the C phase,  $D \rightarrow \infty$ , and for the NC phase,  $D \sim$ 10 nm. Figure 1h presents the CDW domain size maps at select temperatures. At 110 K, the domain size is uniformly > 100 nm, consistent with the C phase. At 187 K, we observe the nucleation of a NC domain (marked with a white arrow), which quickly grows to encompass the entire field of view. We also observe sharp linear features in the D maps. Further analysis reveals that the linear features perfectly align with basal dislocations. Moreover, the NC nucleation event at  $\sim$ 187 K occurs at the intersection of two basal dislocations. The dislocations are evident in virtual dark field maps extracted from the 4D-STEM data, as well as atomic-resolution STEM.

Our experiment shows that basal dislocations act as nucleation centers for the C to NC phase transition, directly linking the flake microstructure to the quantum properties of TaS<sub>2</sub>. Because the dislocations and CDW nucleation occur at sub-surface layers, these results could not have been observed with scanning probe measurements. We will present follow up experiments demonstrating how altered dislocation structures can be used to engineer the CDW transition.

1T-TaS<sub>2</sub> is also of interest due to its non-linear electronic properties: starting in the insulating C phase, if a sufficiently large electric field is applied, TaS<sub>2</sub> rapidly transitions to the metallic NC phase. This behavior is attractive for neuromorphic computing hardware. However, the underlying mechanism of resistive switching remains debated. Does the applied field directly couple to the CDW order parameter and drive switching? Or, does the applied field lead to Joule heating and thermally trigger the transition?

We resolve this question with our *in situ* (S)TEM experimental approach. In Fig. 2a we present *in situ* current vs voltage (IV) sweeps with the maximum applied voltage ranging from 0.5 up to 1.0 V. The data is collected at a base temperature of  $T_0 \sim 110$  K. For voltages  $\leq 0.7$  V, the IV behavior is linear, and *in situ* electron diffraction measurements confirm that the flake remains in the C CDW phase. Conversely, when the applied voltage exceeds  $\sim 0.8$  V, there is a dramatic increase in current. *In situ* electron diffraction shows a CDW transition concomitant with the resistive transition (Fig. 2a insets).

Next, we estimate the local flake temperature based on strain analysis of electron diffraction data collected on the EMPAD-G2. Figure 2b shows the measured strain during each of the voltage ramps. For applied voltages  $\leq 0.7$  V, the measured strain reversibly rises and falls with the applied voltage. We attribute this behavior to lattice expansion during to Joule heating. At the CDW transition at  $\sim 0.8$  V, there is a large and sudden lattice expansion due to CDW-lattice coupling. To determinate the thermal coefficient of expansion  $\alpha$  within the C phase, we perform strain measurements during controlled sample heating, as shown in Fig. 2c. Lastly,

<sup>&</sup>lt;sup>1</sup>Department of Materials Science and Engineering, Cornell University, Ithaca, NY, USA

<sup>&</sup>lt;sup>2</sup>School of Applied and Engineering Physics, Cornell University, Ithaca, NY, USA

<sup>&</sup>lt;sup>3</sup>Kavli Institute at Cornell for Nanoscale Science, Cornell University, Ithaca, NY, USA

<sup>&</sup>lt;sup>4</sup>Present address: Nova Research, Alexandria, VA, USA

<sup>\*</sup>Corresponding author: judy.cha@cornell.edu

we estimate the flake temperature during the IV sweeps assuming  $T = T_0 + \alpha \epsilon$ , where  $\epsilon$  is the measured strain. We find that due to Joule heating, the flake temperature reaches ~200 K immediately prior to resistive switching (Fig. 2d). This temperature increase thermally triggers the C to NC phase transition, giving rise to the nonlinear voltage response.

Thus, with our *in situ* cryogenic and electric biasing experiments, we definitively show that the bias-induced 1T-TaS<sub>2</sub> transition is driven by Joule heating [3]. This finding is important for the design of neuromorphic hardware based on the TaS<sub>2</sub> CDW transition. Additionally, our finding that basal dislocations mediate the C to NC phase transition provides a route to microstructure engineering of quantum materials [4].

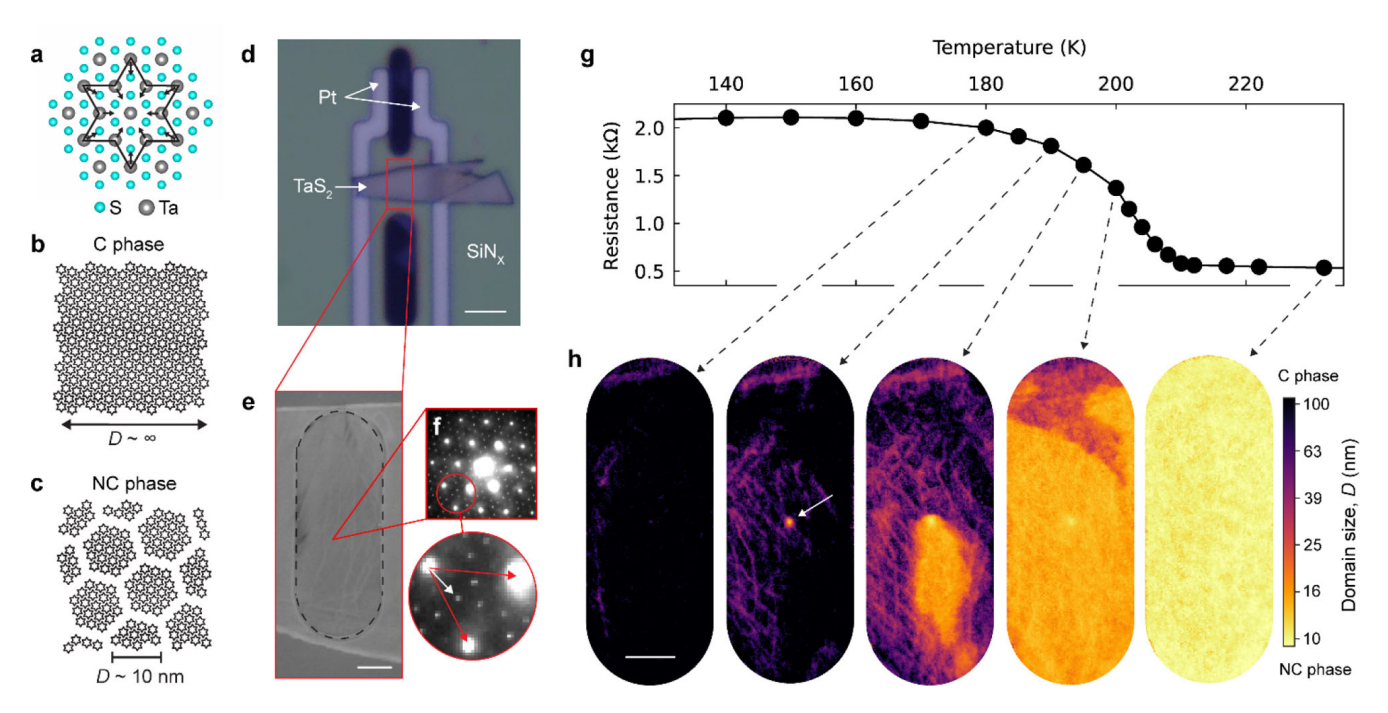


**Fig 1. a.** Plane-view structure of 1T-TaS<sub>2</sub>, showing the star-of-David CDW distortion. **b.** Schematic of the commensurate (C) CDW phase. **c.** Schematic of the nearly commensurate (NC) CDW phase. **d.** Optical image of a TaS<sub>2</sub> flake on the *in situ* chip. Scale bar = 10  $\mu$ m. **e.** STEM annular dark field image of the flake, with the dotted black line marking a through-hole in the SiN<sub>x</sub> support. Scale bar = 1  $\mu$ m. **f.** Extracted diffraction pattern from a 4D-STEM dataset. Lower panel highlights the Bragg lattice vector  $\mathbf{a}^*$  (red arrows) and the CDW  $\mathbf{q}$  vector (white arrow).  $\mathbf{g}$ . Resistance versus temperature for the TaS<sub>2</sub> flake measured within the STEM.  $\mathbf{h}$ . 4D-STEM derived maps of the CDW domain size at select temperatures. Nanoscale nucleation and growth is observed. Scale bar = 1  $\mu$ m.

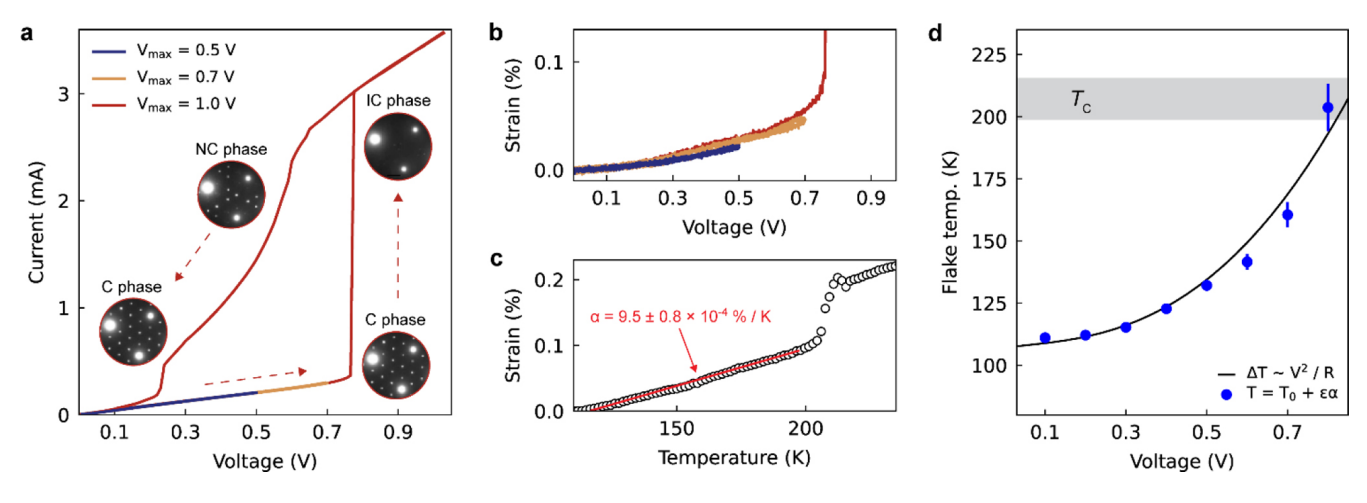


**Fig 2. a.** In situ current vs voltage (IV) sweeps of a 1T-TaS $_2$  flake, with maximum applied voltages of V<sub>max</sub> = 0.5, 0.7, and 1.0 V. When the applied voltage surpasses  $\sim$  0.8 V, the resistance suddenly drops. Insets shown diffraction data collected during the IV sweeps, demonstrating a CDW transition concomitant with the resistance change. **b.** In-plane strain of the TaS $_2$  flake during the IV sweeps. **c.** In-plane strain of the TaS $_2$  flake during from 110 K up to 300 K. A linear fit is used to extract the coefficient of thermal expansion α. **d.** Estimated flake temperature during IV sweeps with V<sub>max</sub> ranging from 0.1 to 0.8 V. T<sub>0</sub> is the base temperature of 110 K,  $\epsilon$  is the measured flake strain, and α is the coefficient of thermal expansion. The solid line provides a fit, assuming the change in temperature from Joule heating is proportional to V<sup>2</sup>/R, where R is the flake resistance. Immediately prior to the resistive switching event, the flake temperature reaches the CDW transition temperature  $T_c$ .

## References

- 1. B Goodge et al, Microscopy and Microanalysis 26 (2020), p. 439. doi.org/10.1017/S1431927620001427
- 2. Thomson, et al, Phys. Rev. B 49 (1994), p. 16899. doi.org/10.1103/PhysRevB.49.16899
- 3. Hart, et al, Nature Communications 14 (2023). doi.org/10.1038/s41467-023-44093-2
- 4. JL Hart and JJ Cha were funded through the Gordon and Betty Moore foundation (EPiQS Synthesis Award). Device fabrication was performed in part at the Cornell NanoScale Facility, a member of the National Nanotechnology Coordinated Infrastructure (NNCI), which is supported by the National Science Foundation (Grant NNCI-2025233). This work made use of the electron microscopy facility of the Platform for the Accelerated Realization, Analysis, and Discovery of Interface Materials (PARADIM), which is supported by the National Science Foundation under Cooperative Agreement No. DMR-2039380, and the Cornell Center for Materials Research Shared Facilities which are supported through the NSF MRSEC program (DMR-1719875). The FEI Titan Themis 300 was acquired through NSF-MRI-1429155, with additional support from Cornell University, the Weill Institute and the Kavli Institute at Cornell.